UDC 53.091

DOI: 10.15372/KhUR20180501

Solid-State Reduction of Oxide Nanoparticles – A New Front of Mechanochemical Technology for Advanced Materials

M. SENNA

Keio University, Japan Faculty of Science and Technology, Hiyoshi, Yokohama (Japan)

E-mail: senna@applc.keio.ac.jp

Abstract

A short review is given on the particular phenomena of abstracting lattice oxygen by conventional hydrocarbon under mechanical stressing. The process can be regarded as a reduction process similar to a traditional hydrometallurgy. However, the mechanochemical process can be regarded as a tool for introducing oxygen vacancies and enables to acquire suboxides or the oxide with lower oxidation number, when we deal with transition metal oxides. Case studies on SiO_2 and V_2O_5, based on our recent experimental studies.

Key words: oxygen abstraction, mechanochemical reduction, solid hydrocarbon, suboxides, oxygen vacancy engineering

INTRODUCTION

Top ranks of the abundance of chemical elements in the earth's crust is, after oxygen at the top, Si, Al, Fe, Ca, Na and K. As a result, world is full of oxides of such metals. Above all, we find SiO_2 everywhere, as quartz crystal in the mountain and white sand on the sea shore. Silica is very stable and takes its feature, depending on the arrangement of its construction units, SiO_4, different polymorphs or amorphous. What happens when it loses oxygen? This simple question triggered this short review.

A great number of natural mineral resources are also oxides, followed by sulphides, just because of their stability. It is not accidental that most of the functional materials are associated with metal oxides. Functionality of the oxide materials, on the other hand, is always combined with some unusual transfer of charge or heat upon some stimuli, may they be thermal, mechanical, electrical *etc*. For those responses, the materials need higher mobility of corresponding species like charge, spin or lattice. Extremely smart cases for those functionalities are associated with strong correlation in condensed matters [1]. For increasing materials functionality including more general mechanical activation, we need excess free energy [2]. This parallels the instabilization of the substances we deal with.

It is generally understood that oxides with multiple oxidation states like those of transition metals, those with their highest oxidation number are most stable. In case of other oxides with a fixed oxidation number, ordinary oxides are more stable than suboxides, where oxygen is deficient from the stoichiometry. Therefore, reduction of the usual oxides is associated with their destabilization and hence, activation.

Reduction of metal oxides is one of the oldest technologies since the Bronze Age. Irrespective of whether pyrometallurgy or hydrometallurgy, their goal is to obtain metals. To improve the properties of oxides, we must stop the reduction process at an appropriate intermediate stage before metallization. For removal of oxygen, we need reductants, to which oxygen has higher affinity than to the metal in the original oxides. Reductants for conventional metal oxides are plenty. Hydrogen or CO represents in the form of a gas. For solid reduc-

tants, we count carbon or metals. The reduction processes are called as carbothermic [3] or metallothermic [4] reactions, respectively.

This short review begins with the concept of mechanochemical reduction, followed by the functionalization of metal oxides, where oxygen vacancies play an important role. Some case studies of mechanochemical reduction to suboxides or to the compounds with lower oxidation number are also given, before concluding remarks and outlooks.

CONCEPT OF *IN SITU* MECHANOCHEMICAL REDUCTION

The present concept is based on the chemical interaction between electrophiles and nucleophiles, which is a textbook issue in the general chemistry. On the surface of oxides, oxygen atoms with varying extent of polarization depending on the composition and structural defects are present. Irrespective of those details, surface of metal oxides is rich in electron densities due to lone pair electrons of oxygen, and hence nucleophilic. Conversely, any hydrocarbon species, irrespective of their phases, are rich in hydrogen atoms, which are polarized toward protons, and hence electrophilic. When those two species come across into contact, a nucleophilic–electrophilic reaction spontaneously takes place. This is associated with the oxygen abstraction from the oxide surface, with simultaneous oxidative decomposition of the hydrocarbon. Simplified schemes are given in Fig. 1. This is what is happening upon milling a mixture of metal oxides and hydrocarbons. Mechanochemical conditions are favourable because the particles are prone to disintegrate, so that the contact points of dissimilar species, oxide and hydrocarbon are spontaneously increase. Upon encounter of these partners, surface species are mutually polarized [5]. This also enhances the necessary charge transfer. Related mechanisms have been extensively explored in the area of heterogeneous catalysis [6]. These methods are also applied to modification of oxides with other anions like F, when the hydrocarbon contains such anionic species [7, 8]. The mechanochemical reduction process mentioned above is a method of introducing oxygen vacancies, which are closely related to a number of functionalities.

FUNCTIONALITY OF OXIDES WHERE OXYGEN VACANCIES PLAY IMPORTANT ROLES

Charge neutralization is one of the starting points of solid state physics. Therefore, when an oxygen ion, O^{2-}, is deleted an oxygen vacancy, V_O, is formed. It is well known that there are three possible charge-states of oxygen vacancies, *i. e.*, neutral (V_O^0), 1+ (V_O^{1+}) and 2+ (V_O^{2+}) [9], corresponding to those with trapped electrons, 2, 1 and 0, respectively [7]. Details of these states are out of scope of the present review. Roles of oxygen vacancies are, however, so diverse and important, that some examples will be given below.

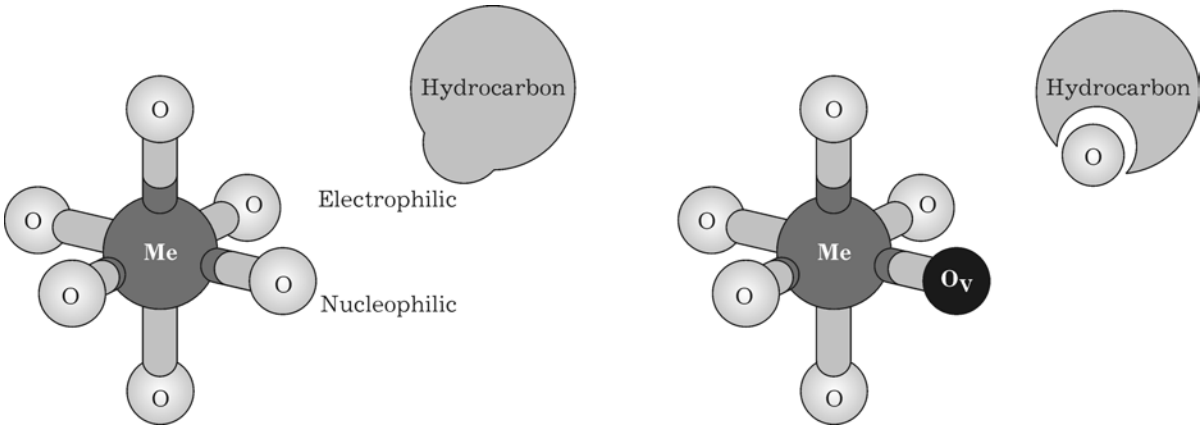

Fig. 1. Scheme of oxygen abstraction from metal oxide by hydrocarbon.

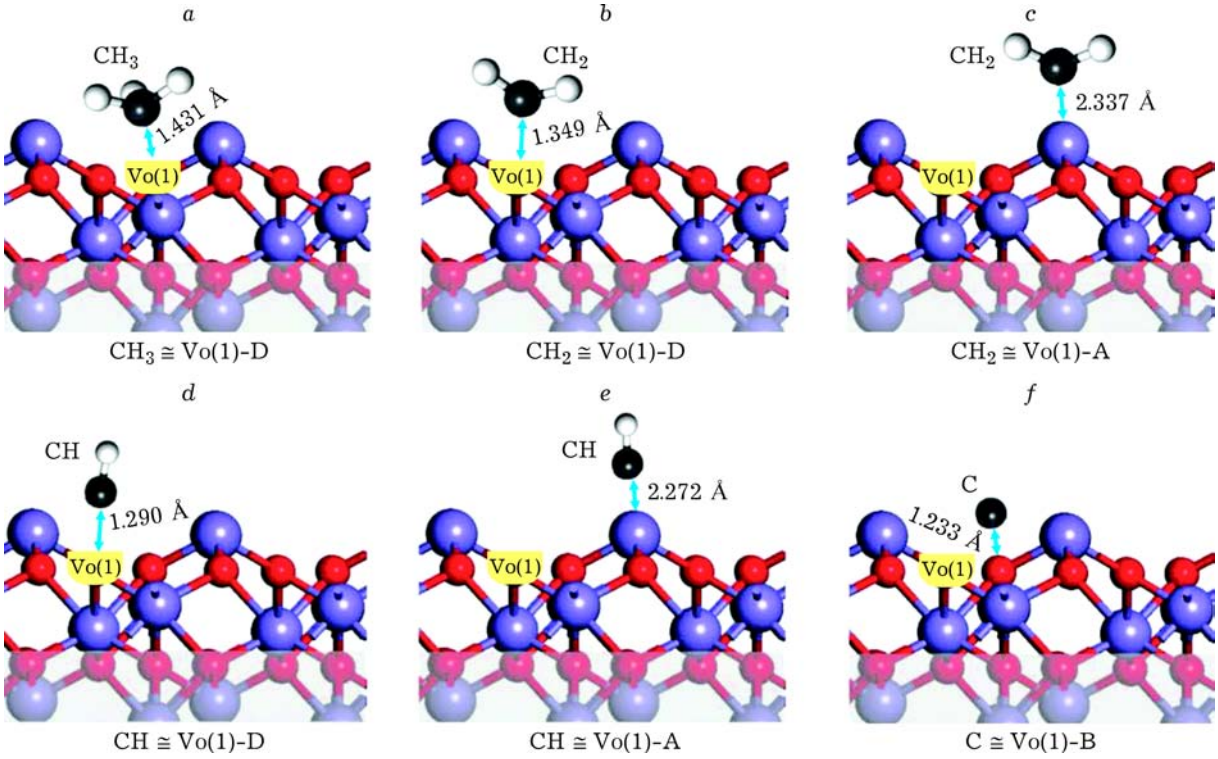

Fig. 2. Most stable CH_x radical adsorption configuration on the reduced α-Fe_2O_3 (001) surface with Vo(1) vacancy. The distance between the C atom and the closest surface atom is indicated. Cited from ref. [10] with permission.

METHANE DECOMPOSITION

Methane is very stable and need extreme conditions to decompose [10]. It is therefore a spontaneous effort to improve catalytic activity for methane decomposition. Cheng *et al.* found that simple iron oxide can decompose methane with the help of oxygen vacancies [11]. Figure 2 is only an example of many others, where the adsorption configurations are demonstrated on the α-Fe_2O_3 (001) surface with stoichiometry and with oxygen vacancies. They confirmed that the adsorption energy of methane decreased significantly by the introduction of oxygen vacancies [11].

OXYGEN REDUCTION

For solid oxide fuel cell (SOFC), oxygen reduction at the cathode is one of the central issues. For NiO as a model substance, Sugiura *et al.* studied the effect of oxygen vacancies on the splitting reaction of surface peroxide ion, which is a rate-determining of oxygen reduction [12]. By an *ab initio* computational calculation, they confirmed that Ni atoms next to the oxygen vacancies are richer with electrons, which can be donated to the adsorbed oxygen, promoting oxygen dissociation. The phenomena can be practiced improving the fuel cell efficiency.

PHOTOCATALYTIC WATER SPLITTING

Water splitting *via* a photocatalytic route is one of the basics of obtaining a clean energy source. For this purpose, tremendous efforts have been paid to make TiO_2 to visible light absorptive [13]. Zhang *et al.* prepared a series of more efficient photocatalysis, CeO_2 with varying concentration of oxygen vacancies [14]. They first found that many important properties like the optical absorption, charge transfer efficiency and catalytic activity are closely related with the concentration of oxygen vacancies. The key mechanism is the decrease in the barrier energy of the rate determining step of water splitting, *i. e.* O–O bond formation and restrain the reverse reaction of O and H [14].

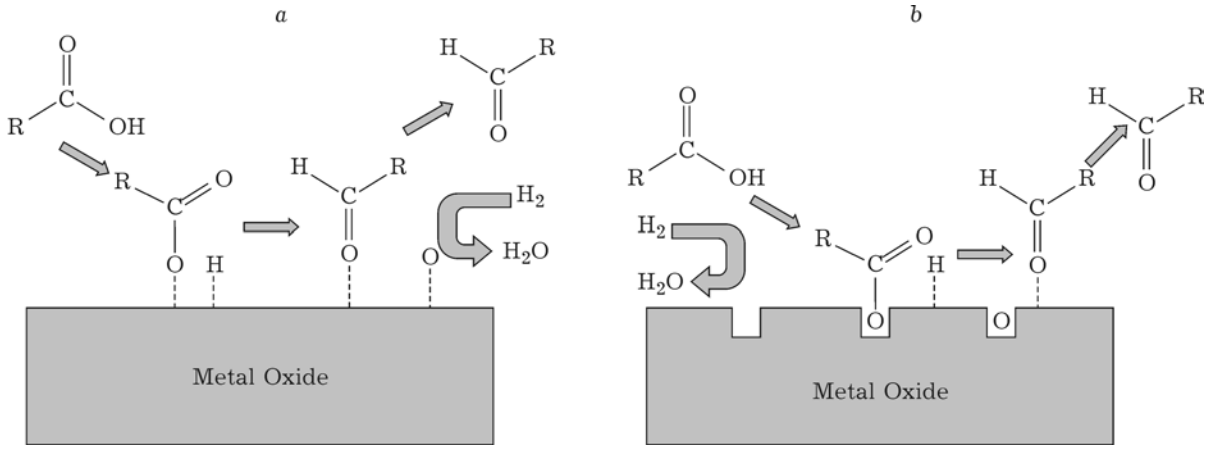

Fig. 3. Possible mechanisms of deoxygenation of bio-oil model compounds over metal oxide: *a* – surface-driven mechanism, *b* – vacancy-driven mechanism.

BIOMASS DEOXYGENATION

Use of biomass is an important alternative of utilizing non-toxic, clean energy sources. For this purpose, selective removal of oxygen is essential to upgrade the biomass-derived molecules. Xiao *et al.* demonstrated another example of making catalysts for the deoxygenation of biomass by using one of the ubiquitous oxides, ZnO [15]. Figure 3 demonstrates a possible mechanism of deoxygenation of bio-oil model compounds over metal oxide. Figure 3, *a* explains the surface-driven mechanism, in which the reactant adsorbs on the surface to react with reducing gas, hydrogen. In contrast, Fig. 3, *b* shows a vacancy-driven mechanism, in which the catalyst facilitates the dissociative adsorption of the reactant through the vacant site on the surface.

EXAMPLES OF MECHANOCHEMICAL REDUCTION

Redox reaction

Šepelák *et al.* [16] reported a solid-state redox reaction from α-Fe_2O_3 and SnO to FeO and SnO_2 by milling their equimolar mixture. In this case, oxygen atoms are transferred unidirectionally from Fe_2O_3 to SnO, so that creation of oxygen vacancies was not monitored. They monitored the process by *ex situ* Mössbauer spectroscopy of ^{57}Fe and ^{119}Sn, as shown in Fig. 4 *a* and *b*, respectively. The figure exhibits for the mixture originally comprising α-Fe_2O_3 and SnO after milling for 20 h. ^{57}Fe Mössbauer spectra reveals 47 % FeO with Fe^{2+}, which did not exist in the starting mixture. Likewise, ^{119}Sn spec-

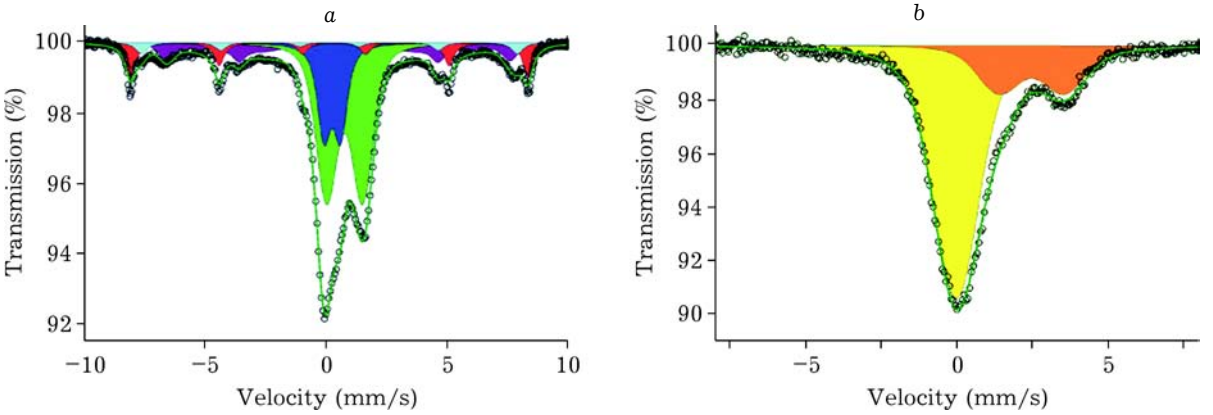

Fig. 4. ^{57}Fe (*a*) and ^{119}Sn (*b*) Mössbauer spectrum of the α-Fe_2O_3 + SnO mixture milled for 20 h. Cited from ref. [15] with permission.

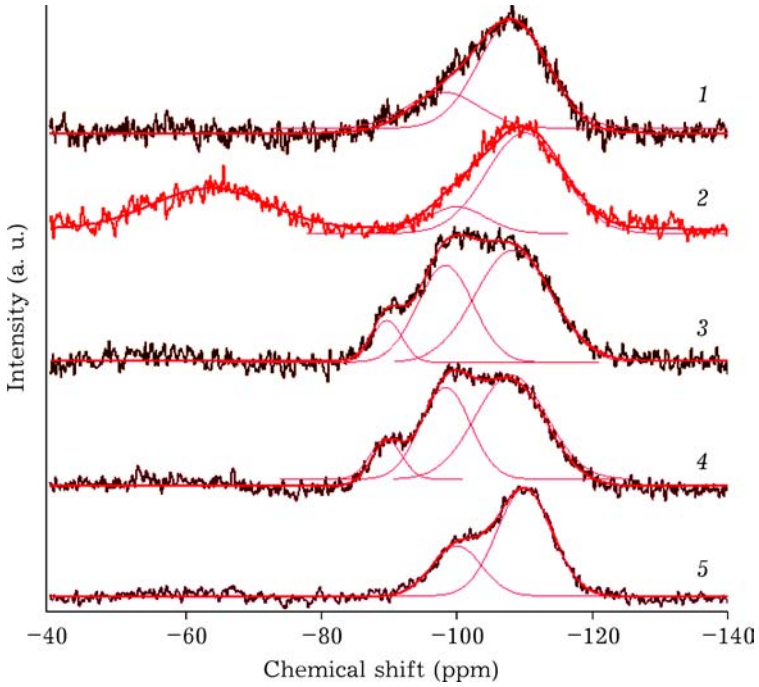

Fig. 5. ^{29}Si MAS NMR spectra of SiO_2, SiO and the mixtures with SiO_2:POL after milling for 3 h: *1* − SiO_2, *2* − SiO, *3* − SiO_2 + PP (9 : 1), *4* − SiO_2 + PE (9 : 1), *5* − SiO_2 + PVDF (9 : 1).

tra revealed 74 % of newly formed Sn^{4+}. These are clear evidences of mechanochemical redox reaction, where reduction of Fe^{3+} and oxidation of Sn^{2+} took place simultaneously

Formation of suboxides from SiO_2

Reduction of SiO_2 nanoparticles are demonstrated and compared in Fig. 5 by means of ^{29}Si magic angle spinning solid state NMR. Out of 5 curves displayed, the top two curves correspond to intact SiO_2 and commercially available nominal SiO, being prepared *via* a conventional thermal reduction route. The bottom 3 curves correspond to the mechanochemical products, where a mixture of silica and 3 different polyolefin powders, *i. e.* polypropylene (PP), polyethylene (PE) and polyvinylidene fluoride (PVDF), respectively. For these 3 curves, the peaks at around −80…−120 ppm are particularly broad as compared with the top two curves. This is an indication of the diversity of the SiO_x units (x = 2, 3 or 4). Their proportion is summarized in Table 1. Coexistence of those states of such states with $x < 4$ is a clear indication of the introduction of oxygen vacancies as a conse-

TABLE 1

Relative intensities (chemical shift) of ^{29}Si MAS NMR signals with different coordination states

Sample/Coordination state	Q^1	Q^2	Q^3	Q^4
Intact SiO_2	0	0	25.29 (98 ppm)	74.71 (108 ppm)
Commercial SiO	0	0	16.74 (100 ppm)	83.26 (110 ppm)
Co-milled with PP	0	8.16 (90 ppm)	35. 49 (98 ppm)	56.35 (108 ppm)
Co-milled with PE	0	9.48 (90 ppm)	34.49 (98 ppm)	56.03 (108 ppm)
Co-milled with PVDF	0	0	29.74 (100 ppm)	70.25 (110 ppm)

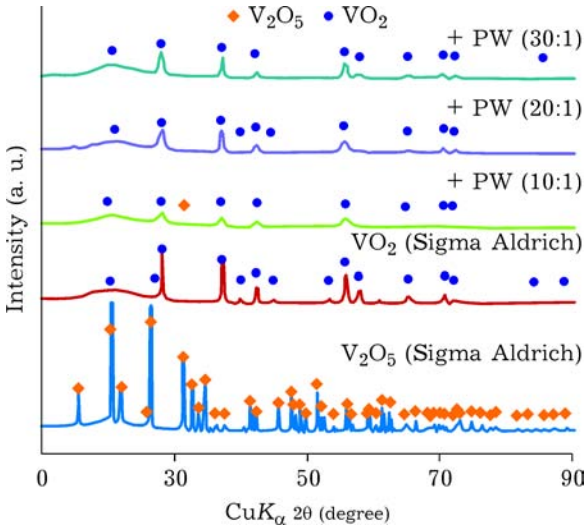

Fig. 6. X-ray diffractograms for fixed milling time (3 h) with varying MRVP [16].

quence of mechanochemical reduction. This was made possible by the oxygen abstraction from the SiO_4 units, with a simultaneous oxidative decomposition of the polyolefins.

Reduction to a stoichiometric oxide with lower oxidation number

As a final example, mechanochemical reduction from V_2O_5 to VO_2 is introduced. This took place when V_2O_5 was milled with paraffin wax (PW) [17]. Unlike the previous example where reduction brought about non-stoichiometric suboxides, the results here exhibit formation of stoichiometric oxide with lower oxidation number.

Figure 6 demonstrates formation of crystalline VO_2 from the mixture of V_2O_5 and PW with their mass ratio (MRVP). With the MRVP larger than 20 : 1, phase pure VO_2 after milling for 3 h (Table 2). VO_2 is known as a material for

TABLE 2

Phase transition temperature and amount of latent heat of the samples for fixed milling time (3 h) with varying V_2O_5/HC ratio, and commercial VO_2 (Sigma Aldrich)

Parameter		+PW (10 : 1)	+PW (20 : 1)	+PW (30 : 1)	VO_2 (Sigma Aldrich)
Transition temperature (°C)	Heating	59.8	58.8	5.3	54.2
	Cooling	69.1	79.6	78.8	66.8
Latent heat (J/g)	Heating	−8	−10.8	−21.6	−17.6
	Cooling	5.5	10.3	20.3	17.9

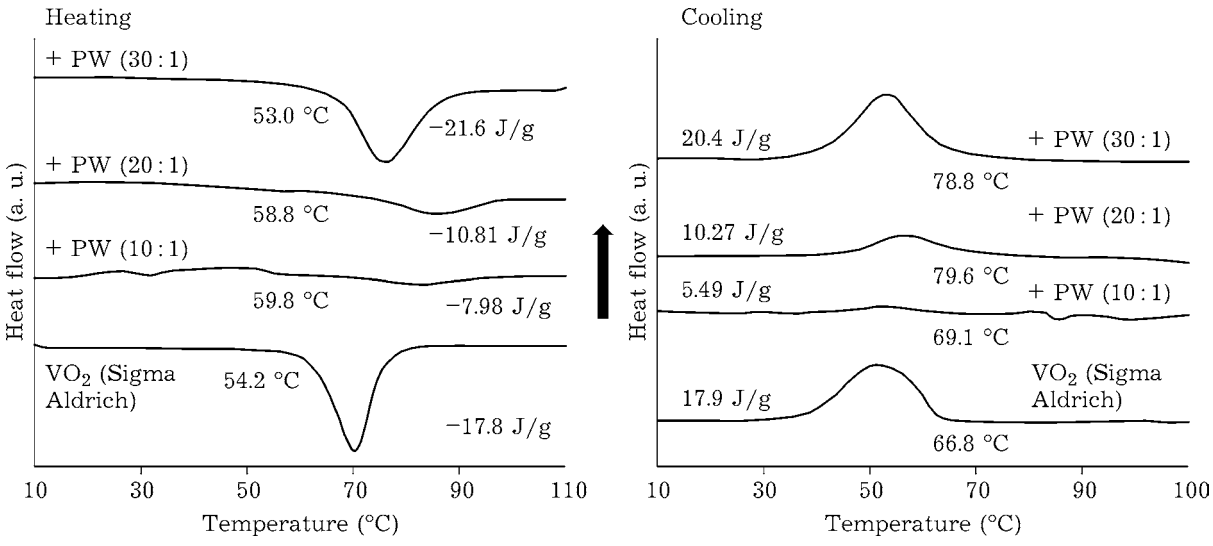

Fig. 7 DSC profiles of the samples for fixed milling time (3 h) with varying MRVP [16].

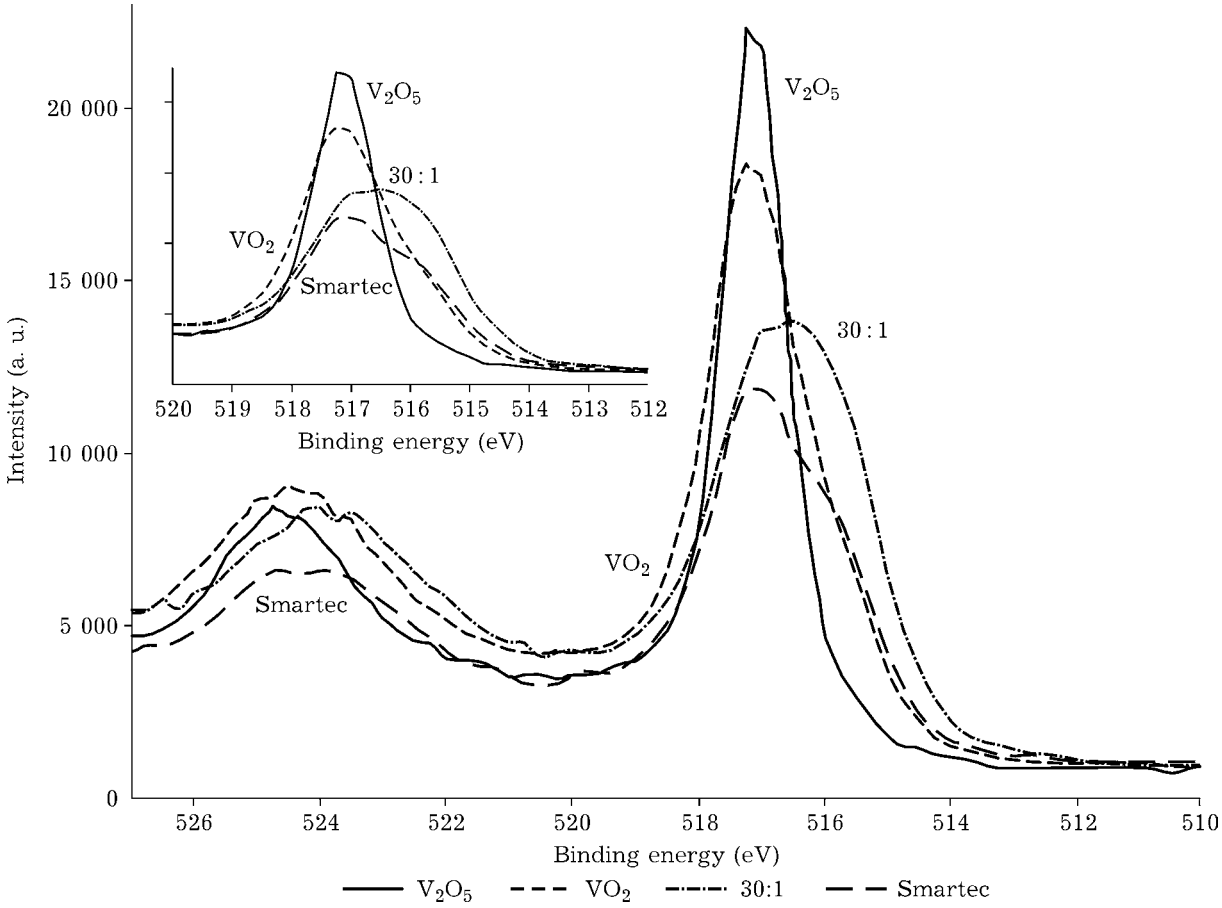

Fig. 8. V 2*p* XPS profiles of topmost surface (0 min etch) [16].

heat storage devices in the form of latent heat during its reversible polymorphic transformation between monoclinic and tetragonal phases at around 68 °C [18].

As shown in Fig. 7, DSC peaks during their phase transformation is larger for mechanochemically reduced VO_2 than commercial product. Despite the commonly understood rules of smaller latent heat with larger lattice imperfection, mechanochemically derived VO_2 in this case exhibits larger latent heat. This is most probably attributed to the stabilization of the reduced cation by neighbouring oxygen vacancies, as a unique XPS profile in Fig. 8 indicates.

CONCLUSION

Mechanochemical reduction of metal oxide fine particles by co-milling with hydrocarbon is based on the principle of nucleophilic–electrophilic reaction and very simple and easy to practice. The reduction begins with formation of oxygen vacancies with simultaneous oxidative decomposition of the hydrocarbon. Unlike conventional thermal or chemical route, co-milling can be conducted under various milling conditions and hence enables to tune the extent of reaction, and hence, control the concentration of the introduced oxygen vacancies. Thus, mechanochemical reduction using hydrocarbon as a reductant has a big potential to modify and functionalize many oxides materials with uniquely stabilized reduced state of metallic cations.

Acknowledgments

The author thanks all the co-workers and co-authors appeared in the case studies cited as references, *i. e.* [7, 8 and 17]. He particularly thanks for the financial supports enabling his research stay in Karlsruhe (Karlsruhe Institute of Technology) and in Kosice (Institute of Geotechnics, Slovak Academy of Sciences, in conjunction with SAIA program of Slovakia).

REFERENCES

1 Kotliar G., Vollhardt D. // Phys. Today. 2004. Vol. 57. P. 53–59.
2 Mohan D. B., and Sunandana S. C. // J. Phys. Chem. B. 2006. Vol. 110. P. 4569–4575.
3 Temuujin J., Senna M., Jadambaa T., Byambasuren D. // J. Am. Ceram. Soc. 2005. Vol. 88. P. 983–985.
4 Okabe T. H. and Sadoway D. R. // J. Mater. Res. 1998. Vol. 13. P. 3372–3377.
5 Busca G. L. V., Ramis G., Escribano V. S. // Mater. Chem. Phys. 1991. Vol. 29. P. 175–189.
6 Meng Y., Genuino H. C., Kuo C. H., Huang H., Chen S. Y., Zhang L., Rossi A., Suib S. L. // J. Am. Chem. Soc. 2013. Vol. 135. P. 8594.
7 Senna M., Šepelák V., Shi J., Bauer B., Feldhoff A., Laporte V., Becker K.-D. // J. Solid State Chem. 2012. Vol. 187. P. 51–57.
8 Senna M., Turianicová E., Zorkovská A., Makreski P., Kaтuchová M., Scholz G., Baláž M., Baláž P., Šepelák V., Hahn H. // J. Nanoparticle Res. 2015. Vol. 17.
9 Kimmel A. V., Sushko P. V., Shluger A. L., Bersuker G. // ECS Trans. 2009. Vol. 19. P. 3–17.
10 Ashik U. P. M., Wan Daud W. M. A., Abbas H. F. // Renewable and Sustainable Energy Rev. 2015. Vol. 44. P. 221–256.
11 Cheng Z., Qin L., Guo M., Fan J. A., Xu D., Fan L. S. // Phys. Chem. Chem. Phys. 2016. Vol. 18. P. 16423–35.
12 Sugiura S., Shibuta Y., Shimamura K., Misawa M., Shimojo F., Yamaguchi S. // Solid State Ionics. 2016. Vol. 285. P. 209–214.
13 Etacheri V., Di Valentin C., Schneider J., Bahnemann D., Pillai S. C. // J. Photochem. Photobiology C: Photochemistry Reviews. 2015. Vol. 25. P. 1–29.
14 Zhang Y.-C., Li Z., Zhang L., Pan L., Zhang X., Wang L., Fazal-e-Aleem A., Zou J.-J. // Appl. Catal. B: Environ. 2018. Vol. 224. P. 101–108.
15 Xiao X., Bergstrom H., Saenger R., Johnson B., Sun R., Peterson A. // Catal. Sci. Technol. 2018. Vol. 8. P. 1819–1827.
16 Šepelák V., Nasr Isfahani M. J., Myndyk M., Ghafari M., Feldhoff A., Becker K. D. // Hyperfine Interactions. 2011. Vol. 202. P. 39–46.
17 Takai C., Senna M., Hoshino S., Razavi-Khosroshahi H., Fuji M. // RSC Adv. 2018. Vol. 8. P. 21306–21315.
18 Morin F. J. // Phys. Rev. Lett. 1959. Vol. 3. P. 34–36.